Geophysical Research Letters

RESEARCH LETTER
10.1029/2018GL077792

Are Bedload Transport Pulses in Gravel Bed Rivers Created by Bar Migration or Sediment Waves?

Blaise Dhont[1] **and Christophe Ancey**[1]

[1] Laboratory of Environmental Hydraulics, École Polytechnique Fédérale de Lausanne, Lausanne, Switzerland

Key Points:
- Alternate bars exhibited stick-slip motion, generating intense bedload pulses
- Episodic bar migration accounted for 36% of the bedload volume carried
- Continuous cycles of pool aggradation and degradation caused the formation and motion of sediment waves

Supporting Information:
- Supporting Information S1
- Movie S1
- Movie S2
- Movie S3
- Movie S4

Correspondence to:
C. Ancey,
christophe.ancey@epfl.ch

Citation:
Dhont, B., & Ancey, C. (2018). Are bedload transport pulses in gravel bed rivers created by bar migration or sediment waves? *Geophysical Research Letters*, *45*. https://doi.org/10.1029/2018GL077792

Received 5 MAR 2018
Accepted 17 MAY 2018
Accepted article online 24 MAY 2018

Abstract Bedload transport exhibits considerable spatial and temporal variability, as reflected by large fluctuations of transport rates. Among the various mechanisms proposed for explaining this variability, bedform migration is often cited as the main cause. We took a closer look at this issue by running long-duration experiments in a gravel bed flume using constant water discharge and sediment feed rates. We monitored bed evolution and measured bedload transport rates at the flume outlet using high-resolution techniques. The bed was initially flat, but within a few hours bedforms consisting of alternate bars and pools had developed. The bars exhibited a stick-slip motion: they were stable for long periods but moved episodically (every 10 hr on average). Their downstream migration produced 36% of the sediment volume transported, mostly in the form of intense pulses. Much of the transport was caused by the displacement of sediment waves from pool to pool.

Plain Language Summary Sediment transport rates show considerable variability with time, even if the water discharge is constant. It has long been realized that rivers develop bed forms such as bars and dunes, which can migrate upward or downward. Their slow motion has thus been viewed as the main cause of fluctuations of sediment transport rates. However, streambeds free of bed forms also experience highly fluctuating sediment transport. We took a closer look at this issue by running a long-duration experiment using a tilted flume filled with gravel. The water discharge and sediment feed rate were kept constant at the flume inlet. Using recent high-resolution techniques, we monitored bed topography and sediment transport rates at the flume outlet. Quickly after the experiment started, a continuous series of bars and pools formed and occupied the entire flume length. In contrast with earlier observations, we noted that these bars mostly stayed at the same place. Every 10 hr on average, they moved downstream, producing bursts of sediment transport. In our experiment, the main source of fluctuations for the sediment transport rates was the cyclic erosion and filling experienced by pools.

1. Introduction

Even the earliest measurements of bedload transport noted that the process exhibited considerable temporal variability, even at constant water discharge (Gomez, 1991). This variability does not resemble what is observed for other physical systems, such as turbulent flows. Indeed, transport rate fluctuations do not follow a Gaussian distribution nor feature short autocorrelation times. They instead display more or less periodic, jigged oscillations (often called *pulses*) and intermittency over short time periods. The origin of this fluctuating behavior has attracted growing attention over the years, with various explanations put forward. Today, the most obvious explanation would seem to be the very nature of bedload transport, which involves the random motion of particles carried by the turbulent water stream (Einstein, 1950). Although the macroscopic consequences of particle agitation at the microscale have been studied theoretically and experimentally (Ancey et al., 2008; Ancey & Heyman, 2014; Ballio et al., 2014; Campagnol et al., 2012; Furbish et al., 2012; Martin et al., 2012; Radice et al., 2009; Redolfi et al., 2018; Roseberry et al., 2012; Singh et al., 2009; Wilson & Hay, 2016), to the best of our knowledge, no clear connection between particle agitation and pulses has been demonstrated. While particle agitation is usually considered to be noise and inhibit structure formation, there are instances in which nonlinear instability mechanisms induced by noise generate coherent structures. For instance, random water waves can create rogue waves, which can be seen as giant *pulses* distinct from the other waves (Dysthe et al., 2008). While particle agitation has been proposed for explaining bedform formation

(Ancey & Heyman, 2014), there is no evidence that it also generates bedload transport pulses. Another possible explanation for pulses is related to bedform migration, possibly associated with a number of processes (e.g., local aggradation and degradation and sediment waves) (Ashmore, 1991; Gomez et al., 1989; Hoey & Sutherland, 1991). Heuristic models for sand dunes have suggested relating sediment transport rates to dune features (velocity and height; Hamamori, 1962; Simons et al., 1965), but because river bedforms are far more complex (Aberle et al., 2012; Guala et al., 2014; Keylock et al., 2014; Lanzoni, 2000), the connection between bedform and transport rate needs further elaboration. A third scenario highlights the part played by grain sorting (Bacchi et al., 2014; Cudden & Hoey, 2003; Ghilardi et al., 2014; Iseya & Ikeda, 1987; Recking et al., 2009; Saletti et al., 2015). However, although this can explain why transport rate fluctuations are exacerbated by grain sorting (especially due to a number of concomitant processes such as bed armoring and partial transport), this scenario alone cannot explain the occurrence of bedload transport pulses. In natural environments, other causes (e.g., varying sediment supply and flow conditions) are likely, but again, they cannot be the sole mechanisms of pulse generation because pulses are ubiquitous in the laboratory and nature, under various flow conditions.

To shed light on the issue of pulse generation, we devised a simple experiment in which we monitored bed morphology and sediment transport rates under steady state conditions (i.e., at constant water discharge and sediment supply rates). The experimental campaign differed from earlier studies because we ran the experiments over very long times (more than 500 hr) and focused on gravel transport in a steep flume with low transport rates. Flow conditions were thus close to supercritical; alternate bars and pools formed quickly, and sediment transport exhibited considerable temporal and spatial variability. We used modern techniques allowing us to monitor bedload transport rates and bed morphology at high temporal resolutions, which gave us the opportunity to study bedload transport over a wide range of timescales (from minutes to days). Supporting information provides additional information on the experimental procedure and analysis, together with four movie excerpts.

2. Methods

We used a 19-m-long, 60-cm-wide flume, with its bottom inclined at 1.6% to the horizontal. The bed was composed of well-sorted natural gravel (mean diameter 5.5 mm, standard deviation 1.2 mm). Initially, the bed was flat. As planar beds are unstable, bedforms (here, alternate bars and pools) developed along the bed, causing a slope adjustment over a transient phase of duration $t_a \sim 710$ min. The time-averaged bed slope (over the run duration) was 1.49%, whereas its range of variation was 1.2%–1.8%.

Water discharge was controlled by a recirculating pump. A hopper stored the gravel and released a fixed amount of it per unit time, which was taken to the flume inlet on a conveyor belt. See Movie S1 and the supporting information for further information.

Water discharge at the inlet was $Q_w = 15$ L/s (uncertainty 0.01 L/s); the gravel feed rate was $Q_{in} = 5.0$ g/s. Feed rate time variations could be as high as 10%. Water discharge and feed rates were selected during preliminary tests in order to generate a bed slope that was fairly close to equilibrium (as will be demonstrated later, the notion of bed equilibrium and the precise meaning of *close to* call for further explanations). Other flow conditions were also investigated (Dhont, 2017) but are not reported here. The experiment ran for 568 hr. The mean Froude number was close to unity, as is often the case for these kinds of conditions (Grant, 1997). The flow depth h was 4 cm on average but much deeper in the pools ($h \sim 10$ cm). The mean flow velocity was close to 1 m/s. By and large, the Shields number ranged from 0.05 to 0.1, corresponding to incipient or weak particle transport.

The bedload transport rate was measured using six accelerometers (Dhont et al., 2017). Instantaneous transport rates were averaged over a time step $\Delta t = 1$ min. Subsequent analyses were based on these time-averaged values. The bedload transport rate averaged over the whole run duration was $\bar{Q}_s = 4.82$ g/s. Although this value did not exactly match the feed rate Q_{in}, we observed neither noticeable aggradation nor degradation in the long run, and as time variations in the feed rate Q_{in} could reach 10%, we estimated that the two rates were reasonably close to being considered equal. Every 10 min, we measured flow depth and bed topography using ultrasonic probes and image processing (Visconti et al., 2012), respectively. The absolute uncertainties of flow depth and bed elevation were 0.5 mm and 1 cm, respectively.

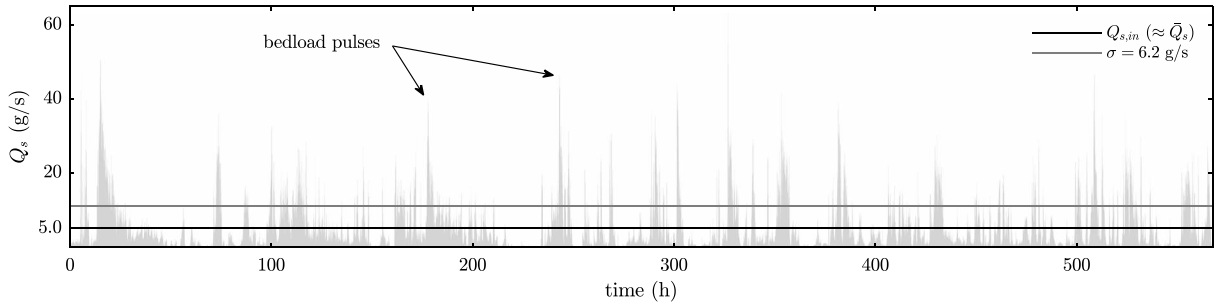

Figure 1. Bedload transport rate Q_s as a function of time. The black horizontal line represents the sediment feed rate $Q_{in} = 5$ g/s, and the thin gray line above it shows the value $\bar{Q}_s + \sigma$, where σ denotes the standard deviation of the transport rate.

3. Fluctuations of the Bedload Transport Rate

Figure 1 shows the time variation in the bedload transport rate (averaged over time periods of $\Delta t = 1$ min, measured at the flume outlet, and including $n = 34{,}050$ values). A number of interesting features deserve attention. First, we note that our time series differed from those observed in many physical systems under steady state conditions, in which the key variables gently fluctuate around mean values. Here we observe a series of pulses separated by periods of low activity (possibly with no transport over short time periods). The time-averaged transport rate $\bar{Q}_s = 4.82$ g/s was not the mode (it did not represent the most frequent state of the system). The intermittent nature of the time series gives the impression that there was no well-defined equilibrium state.

Second, we noticed large fluctuations of Q_s. Indeed, a few times during the run duration, the ratio $Q_s/\bar{Q}_s$ exceeded 12. Over the entire run duration, the coefficient of variation (i.e., $\sigma/\bar{Q}_s$, with $\sigma = 6.2$ g/s the standard deviation of Q_s) was about 120%. Two functions are commonly used for characterizing stationary stochastic processes: the probability distribution and the power spectrum. In Figure 2a, we plot the empirical probability density function (histogram) of Q_S together with two candidate probability distributions recently proposed to describe transport rate fluctuations under steady state conditions. Turowski (2010) used a statistical model derived from the normal distribution, called the Birnbaum–Saunders distribution, whereas Ancey et al. (2008) and Ancey and Heyman (2014) developed a theoretical framework based on Markov jump processes, which show that the number of moving particles follows a negative binomial distribution (see the supporting information). Both distributions have the same number of parameters, and these were fitted to the data using the method of moments. They matched the empirical distribution for $Q_s > 5$ g/s, but they failed to capture the fluctuation distribution in the limit of $Q_s \to 0$. The Birnbaum–Saunders distribution predicts that Prob $(Q_s = 0) = 0$, whereas the empirical probability takes a nonzero value at $Q_s = 0$. The theoretical prediction proposed by Ancey et al. (2008) overestimates the value of this probability, and its poor performance may be attributed to the absence of well-defined equilibrium state. Figure 2b shows the power spectrum $P(Q_s)$. In the low-frequency domain, the spectrum is flatter but exhibits a few bumps. It is unclear whether this should be interpreted as white noise or as the signature of another scaling (e.g., $P \propto f^{-1/2}$ could fit the data roughly). At higher frequencies, the power spectral density decreases as $f^{-3/2}$ with increasing frequency f. The cutoff frequency is about $f_c \sim 30$ μHz (this defines a characteristic time $t_c = f_c^{-1} \sim 10$ hr). We failed to find an explanation for the $-3/2$ slope. A similar slope was found for other flow conditions (Dhont, 2017) or when we focused on shorter periods of time during which no bar migration was observed (see the supporting information).

Third, the intermittent nature of the time series pushed us to take a closer look at the pulse features. Whereas multifractal analysis has become a classic tool for that purpose (González et al., 2017; Singh et al., 2009), we used a simpler method. Let us consider the threshold $Q_{\text{thres}} = 2Q_{s,in} = 10$ g/s. A pulse is defined as a continuous set of transport rates Q_s, which starts at time t_i such that $Q_{s,i} > Q_{\text{thres}}$ and $Q_{s,i-1} < Q_{\text{thres}}$, with $1 \leq i \leq n$ an index. This pulse ends at time t_k such that $Q_{s,k} < Q_{\text{thres}}$and $Q_{s,k-1} > Q_{\text{thres}}$. The pulse duration is thus $d_p = (k - i)\Delta t$. For each pulse j, we can determine a peak value $Q_{s,\max}(j)$ and the time $\delta t(j)$ to the next pulse. We found $n_p = 613$ pulses in our times series, and this large number made it possible to infer some of the statistical properties of those pulses. Figure 3a shows that the peak value $Q_{s,\max}$ varied smoothly and slowly, with the pulse occurrence frequency f_p: $Q_{s,\max} \propto f_p^{-3/10}$. However, we also noted a slight change in behavior at the cutoff frequency. The slow decrease in $Q_{s,\max}$ with f_p confirmed that large fluctuations were quite frequent.

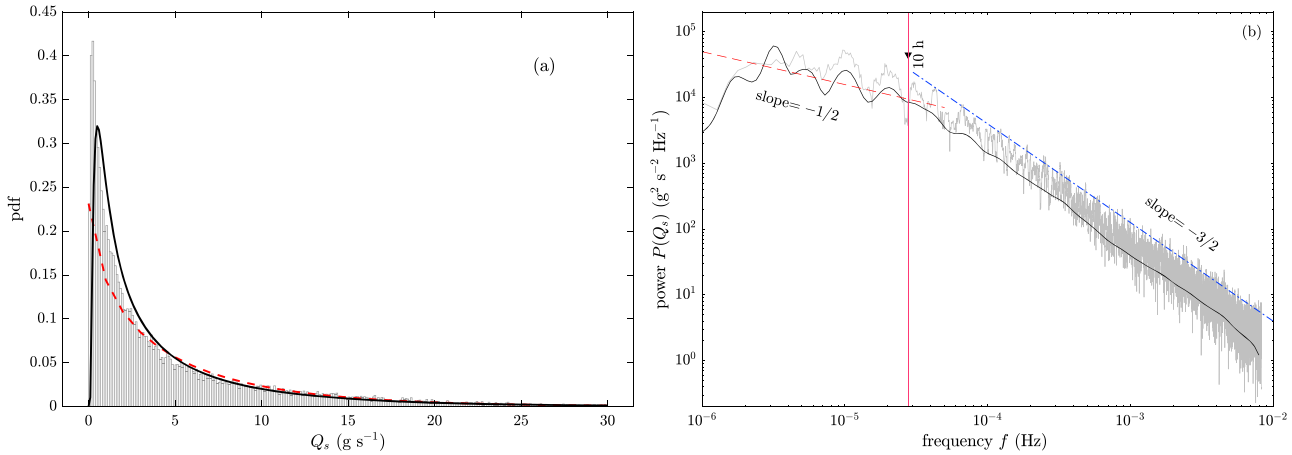

Figure 2. (a) Empirical probability density function of the bedload transport rate (only rates $Q < 30$ g/s are shown). The black solid line shows the Birnbaum-Sanders distribution (Turowski, 2010), whereas the red dashed line approximates the probability distribution inferred by Ancey and Heyman (2014). See the supporting information for further information. (b) Multitaper spectrum (gray) and wavelet spectrum (black) of the bedload transport rates. The vertical line indicates the cutoff frequency $f_c \sim 30$ μHz (and associated characteristic time $t_c = f_c^{-1} \sim 10$ hr).

The peak value was not well correlated with the duration, that is, large values could be observed for pulses of all durations. Surprisingly, as shown in Figure 3b, the pulse volume varied almost linearly with the pulse duration, with little data scattering around the mean trend. Remarkably, this means that the bedload transport rates, when averaged over the pulse duration, were almost constant across pulses. The mean pulse duration was fairly short ($d_m = 510$ s), and contrary to the peak value and the interpulse waiting time, the probability distribution was not heavy tailed. As shown in Figure 3c, a lognormal distribution matches the empirical probability distribution of d_p. Figure 3d reveals the complex behavior for the interpulse waiting time δt. For $f_p > f_c$, the waiting time varied as $\delta t \propto f_p^{-9/4}$, whereas at low frequencies, the variations were 10 times slower: $\delta t \propto f_p^{-1/3}$.

4. Bed Morphology and Bedload Transport Pulse

Soon after the flow was turned on (i.e., within 10 hr), a row of alternate bars and pools developed along the entire length of the flume, leading to a bed morphology composed of three bars and two to three pools. Although the time-averaged bedload transport rate $\bar{Q}_s(T) = T^{-1} \int_{t_0}^{t_0+T} Q_s(t)\mathrm{d}t$ neatly converged to a steady state value for integration times T in excess of $T_c = 225$ hr (see Figure 4a), there was apparently no clear evidence that the bed reached equilibrium. A seemingly stable equilibrium configuration could be observed for tens of hours, but it would eventually fall apart within a few tens of minutes. In the initial phase, during which the bedload transport rate tended to its steady state value ($t < T_c$), the bed volume variation ΔV was mostly negative, suggestive of bed degradation (ΔV was computed at time t as $\Delta V = \int_0^t (Q_{s,in} - Q_s)\mathrm{d}t'/\rho_b$, where $\rho_b = 1{,}420$ kg/m^3 is the bed bulk density). For $t > T_c$, bed aggradation occurred ($\Delta V > 0$). An unequivocal determination as to the cause of this behavior is difficult. It is tantalizing to *detrend* the signal $\Delta V(t)$ (i.e., remove the linear trend) to determine the trend around which the signal fluctuates. This would mean that the process of bed slope adjustment had not been completed within 600 hr and took place over timescales much longer than T_c. Jerolmack and Paola (2010) suggested a much longer characteristic timescale here: $T_c \sim \rho_b L^2/Q_{s,in} = 3.6$ years, which means that a steady state would be hard to achieve at the laboratory scale using a low sediment feed rate. However, drawing any firm conclusions about the fluctuation pattern, given the scale of the laboratory system, remains difficult. In a long flume, minute changes in bed elevation may entail relatively large fluctuations in V. If we cover the flume surface with a layer one particle diameter thick, we obtain a scaled volume $\Delta V/V_m = 10.5$, which is larger than the observed range of variation in Figure 4.

By monitoring bed evolution, we were able to relate bedload transport to local changes in the bed. A striking feature of our experiments was the stick-slip behavior of bars: the bars did not move continuously, but intermittently. They mostly stayed in the same place, but every 10 hr, on average, they moved downstream by 1.4 m. The mean displacement duration was 1.7 hr. Another curious phenomenon was the inversion between

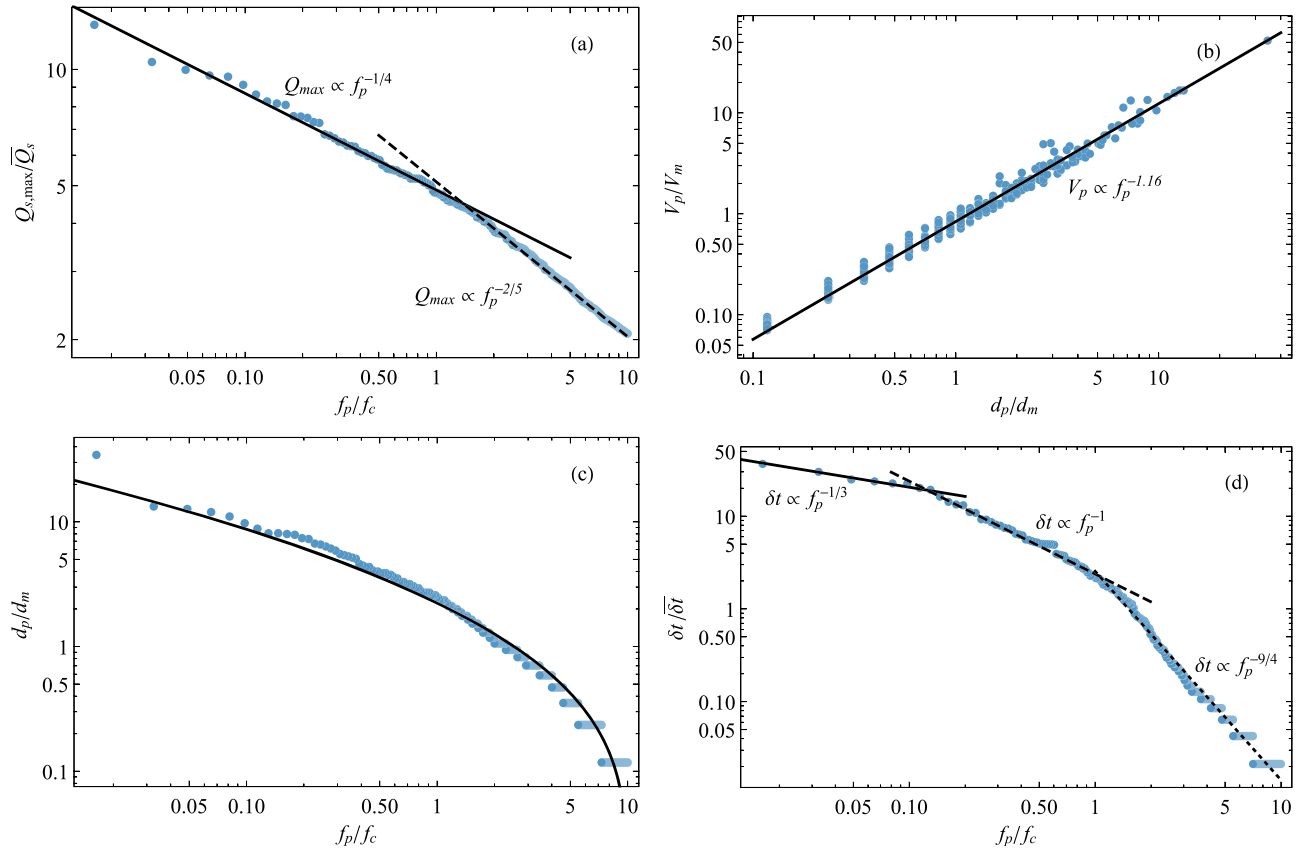

Figure 3. (a) Variation in the peak value of the bedload transport rate $Q_{s,\max}$ with the pulse frequency $f_p(j) = (1 - j/(n_p + 1))n_p/n/60$ and $1 \le j \le n_p$. The values are scaled by the mean transport rate $\bar{Q}_s$ and the cutoff frequency $f_c = 30$ μHz. The solid line shows the trend $Q_{s,\max} \propto f_p^{-1/4}$, whereas the dashed line shows $Q_{s,\max} \propto f_p^{-2/5}$. (b) Variation in the pulse volume with the pulse duration d_p. The variables are scaled using the measured mean pulse volume and duration: $V_m = 6$ l (i.e., a mass 8.52 kg and a bulk density 1,420 kg/m^3) and $d_m = 510$ s. The solid line shows the nonlinear fit $V_p = 0.83V_m(d_p/d_m)^{1.16}$. (c) Variation in the pulse duration with the occurrence frequency. The solid line shows the lognormal distribution $\frac{1}{2}\text{erfc}\left((\alpha - \ln d_p)/(\sqrt{2}\beta)\right)$, with parameters $\alpha = 1.28$ and $\beta = 1.31$. (d) Variation in the interpulse waiting time with pulse frequency. The various scales are shown in the plot. The values are scaled by the mean waiting time $\delta\bar{t} = 2{,}817$ s and cutoff frequency f_c.

pools and bars: when migrating, a bar usually stopped at the pool downstream of it. To illustrate this process, we plotted the spatiotemporal evolution of the two lateral boundaries in Figure 5. More specifically, we measured bed elevation $b(x, y, t)$ along a line parallel to the flume and $y = 5$ cm away from the sidewall. This was repeatedly measured every 10 min. We then aggregated row $b(x_i, y, t_j)$ to form the matrix shown in Figure 5. Movie S2 shows an animation of the two longitudinal bed profiles. Bars were easily identified as their elevation remained stable over time, whereas pools underwent cycles of aggradation and degradation. The right profile in Figure 5 shows that at time $t = 460$ hr, there were two bars located at $x = 9$ m and $x = 1$ m. The former moved at time $t = 490$ hr, then at $t = 510$ hr, whereas the latter moved at $t = 500$ hr and was replaced by a pool. Bar migration caused intense sediment transport. By relating bed evolution and bedload transport time series, we found that 60% of the highest peaks (those which exceeded $6Q_{s,in}$ in Figure 1) were generated by bar migration, but only 20% of pulses (with $Q_s \ge 2Q_{s,in} = 10$ g/s) were triggered by this migration. All in all, bar migration was associated with 36% of the total mass displacement. There can be no dispute that bar migration created bedload pulses, but these were not the main processes in our experiment in terms of their frequency of occurrence and the volumes transported by pulses.

We sought out another mechanism. A closer look at the pools revealed that they underwent continuous cycles of aggradation and degradation, whose signatures were reflected in Figure 5 by the jiggling behavior of bed elevation (of the order of a few centimeters). When cross-correlating the bedload transport rate Q_s and the pool elevation, we found a correlation coefficient of about 0.68 (over a period of 120 hr during which no bar migration was observed), demonstrating that much of the variation in Q_s was caused by changes in the bed

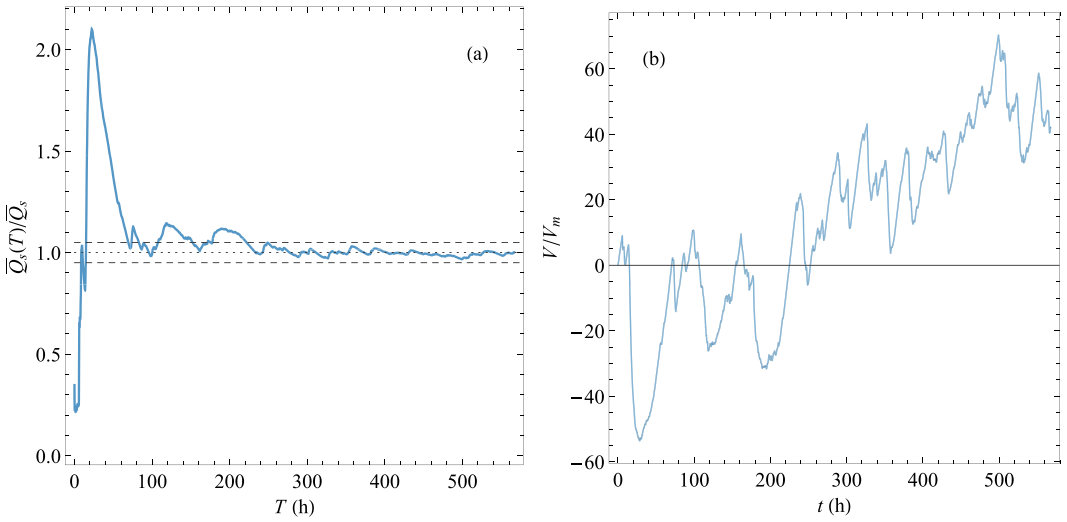

Figure 4. (a) Variation in the time-averaged bedload transport rate $\bar{Q}_s(T) = T^{-1}\int_{t_0}^{t_0+T} Q_s(t)dt$ with integration time T and starting time $t_0 = 0$. The rate has been put to scale using the mean value $\bar{Q}_s = 4.82$ g/s. The dashed lines represent the value $\bar{Q}_s(1 \pm 0.05)$, whereas the dotted line shows the mean value $\bar{Q}_s$. (b) Time variation in the bed volume relative to its initial state ($\Delta V = 0$ at time $t = 0$). Volumes have been put to scale using the mean pulse volume $V_m = 6$ l.

elevation in the pool just upstream of the flume outlet. The cross-correlation analysis between Q_s and the bed elevation of the most upstream pool (11 m away from the flume outlet) led to correlation coefficients as high as 0.67 for a time lag of 70 min. In other words, it took about 1 hr for the material eroded from the upstream pool to reach the flume outlet. The low displacement velocity (2.6 mm/s) did not reflect the actual particle velocity (50 times quicker). Indeed, when particles moved, they had to cross pools. These usually behaved as sediment traps, causing the particles arriving from upstream to come to a halt. Sediment accumulation induced a local slope increase (aggradation) and, presumably, when the slope became too steep, it gave way (degradation) and released grains, which moved down to the next pool. As sediment transport was mediated by pools, motion often took a coherent form: particles mostly moved in clusters, and during the degradation

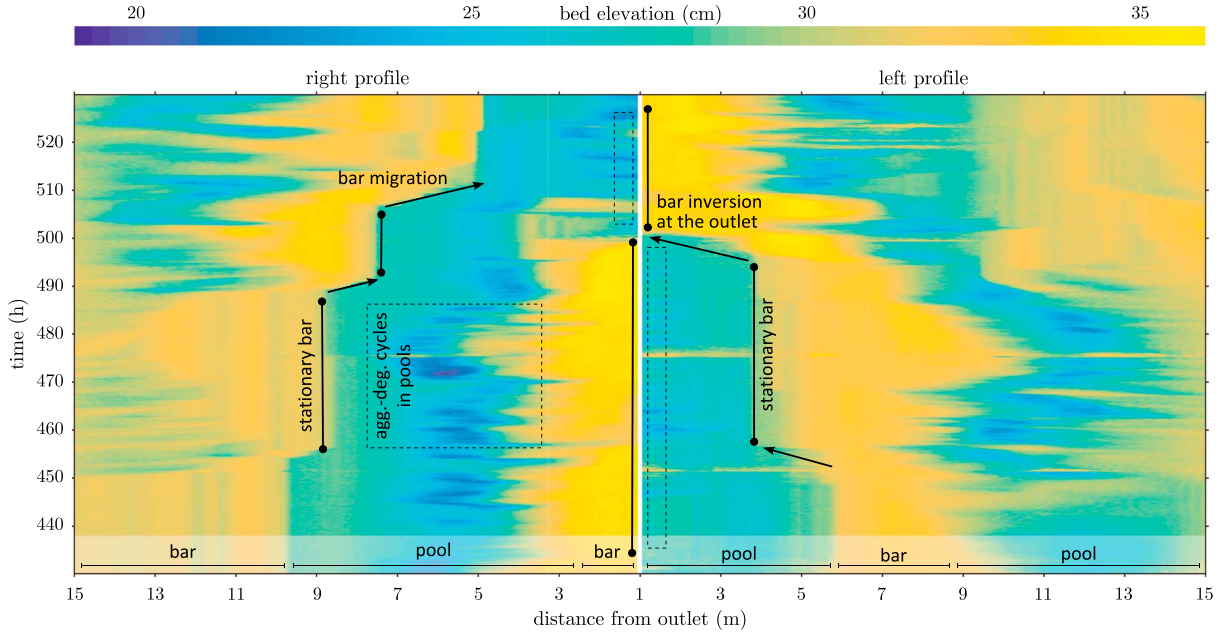

Figure 5. Spatiotemporal evolution of the bed's right and left profiles during a 100-hr sample of the experiment. The two profiles are plotted symmetrically with respect to the flume outlet, which corresponds to the center of the figure. Bars migrated episodically in the downstream direction, and pools underwent cycles of aggradation and degradation as shown by the continuous but limited fluctuations in their elevation.

cycle, we also observed that narrow streams of grains were ejected from the pool. The stream head came quickly to a halt, forming a shallow carpet of grains along the bed (see Movie S3). The incoming grains rolled over this carpet and gathered at its downstream end. The progressive accumulation of grains gave rise to a *sediment wave* as it was described by Lisle (2004), among others, that is, "a disturbance in the interactions between flow, channel topography, and the transport of bed material." On rare occasions, particle migration occurred in the form of a bedload sheet, that is, a large transport of particles moving downstream *en masse*. An animation was created using the bed scans (see Movie S4), and it clearly shows the complex pattern of transient bedforms created by sediment and erosion waves. In this movie, it is worth noting the differences between the wave dynamics in the initial adjustment phase ($t < T_c = 225$ hr) and in the pseudoequilibrium phase ($t > T_c$). In the latter, three pools formed (instead of two), and bed disturbances were much shorter.

5. Concluding Remarks

In this letter, we have studied how bedforms and bedload transport rates were related. In contrast with the mainstream view of bar migration, we found that bars exhibited stick-slip behavior: they mostly stayed in the same position, but at irregular time intervals they suddenly moved downstream, often coming to a halt in the position occupied by a downstream pool. Avalanches on downstream slope faces were the most frequent scenarios leading to bar collapse. This instability occurred every 10 hr on average. This characteristic time plays a key part in the dynamics of sediment transport (see Figures 2 and 3). When the most upstream bar was set in motion, it sent out streams of grains, which in turn contributed to destabilizing the bars downstream, in a domino-like effect. The majority (but not all) of bedload pulses were caused by bar migration: 60% of the intense pulses (i.e., those satisfying $Q_s > 6\bar{Q}_s$) were due to bar migration. If we take a lower threshold, for example, by considering all pulses whose peak values exceeded $2\bar{Q}_s$, then only 20% of pulses could be attributed to bar migration; the rest resulted from sediment waves sent out by pools. Bar migration was thus not the main process at work since 67% of the sediment volume was transported during periods with no bar displacement. Correlation analysis demonstrated that much of the transport was driven by aggradation and degradation cycles in the pools. Pools behaved like buffer zones that stored sediment and sent out clusters of grains sporadically. This gave rise to sediment waves that propagated downward slowly and created many of the bedload transport rate fluctuations.

With regard to the present study, we do not know whether the bar's stick-slip motion is specific to our setting or is a more general feature that has thus far gone unnoticed. Although the part played by bar migration and pool aggradation and degradation in bedload transport rate fluctuations has long been recognized, we know of no study quantifying their respective roles. The present letter provides preliminary quantifications.

Acknowledgments
The authors acknowledge the support of the Swiss National Science Foundation (grant 200021_129538). The script and data used for computing Figure 1 are available from the figshare data repository: https://doi.org/10.6084/m9.figshare.6264758. We thank David Furbish and another reviewer for their astute suggestions and constructive criticisms.

References

Aberle, J., Coleman, S., & Nikora, V. (2012). Bed load transport by bed form migration. *Acta Geophysica*, *60*, 1720–1743.
Ancey, C., Davison, A. C., Böhm, T., Jodeau, M., & Frey, P. (2008). Entrainment and motion of coarse particles in a shallow water stream down a steep slope. *Journal of Fluid Mechanics*, *595*, 83–114.
Ancey, C., & Heyman, J. (2014). A microstructural approach to bed load transport: Mean behaviour and fluctuations of particle transport rates. *Journal of Fluid Mechanics*, *744*, 129–168.
Ashmore, P. (1991). Channel morphology and bed load pulses in braided, gravel-bed streams. *Geografiska Annaler. Series A, Physical Geography*, *73*, 37–52.
Bacchi, V., Recking, A., Eckert, N., Frey, P., Piton, G., & Naaim, M. (2014). The effects of kinetic sorting on sediment mobility on steep slopes. *Earth Surface Processes and Landforms*, *39*, 1075–1086.
Ballio, F., Nikora, V., & Coleman, S. (2014). On the definition of solid discharge in hydro-environment research and applications. *Journal of Hydraulic Research*, *52*, 173–184.
Campagnol, J., Radice, A., & Ballio, F. (2012). Scale-based statistical analysis of sediment fluxes. *Acta Geophysica*, *60*, 1744–1777.
Cudden, J., & Hoey, T. B. (2003). The causes of bedload pulses in a gravel channel: The implications of bedload grain-size distributions. *Earth Surface Processes and Landforms*, *28*, 1411–1428.
Dhont, B. (2017). Sediment pulses in a gravel-bed flume with alternate bars (PhD thesis), École Polytechnique Fédérale de Lausanne, Lausanne.
Dhont, B., Rousseau, G., & Ancey, C. (2017). Continuous monitoring of bedload transport in a laboratory flume using an impact sensor. *Journal of Hydraulic Engineering*, *143*, 04017005-1–04017005-10. https://doi.org/10.1061/(ASCE)HY.1943-7900.0001290
Dysthe, K., Krogstad, H. E., & Müller, P. (2008). Oceanic rogue waves. *Annual Review Fluid Mechanics*, *40*, 287–310.
Einstein, H. (1950). The bed-load function for sediment transportation in open channel flows (Technical Report No. 1026). US: United States Department of Agriculture.
Furbish, D., Haff, P., Roseberry, J., & Schmeeckle, M. (2012). A probabilistic description of the bed load sediment flux: 1. Theory. *Journal of Geophysical Research*, *117*, F03031. https://doi.org/10.1029/2012JF002352
Ghilardi, T., Franca, M., & Schleiss, A. J. (2014). Period and amplitude of bedload pulses in a macro-rough channel. *Geomorphology*, *221*, 95–103.
Gomez, B. (1991). Bedload transport. *Earth Science Reviews*, *31*, 89–132.

Gomez, B., Naff, R., & Hubbell, D. (1989). Temporal variations in bedload transport rates associated with the migration of bedforms. *Earth Surface Processes and Landforms*, *14*, 135–156.
González, C., Richter, D., Bolster, D., Bateman, S., Calantoni, J., & Escauriaza, C. (2017). Characterization of bedload intermittency near the threshold of motion using a Lagrangian sediment transport model. *Environmental Fluid Mechanics*, *17*, 111–137.
Grant, G. (1997). Critical flow constrains flow hydraulics in mobile-bed streams: A new hypothesis. *Water Resources Research*, *33*, 349–358.
Guala, M., Singh, A., BadHeartBull, N., & Foufoula-Georgiou, E. (2014). Spectral description of migrating bed forms and sediment transport. *Journal of Geophysical Research: Earth Surface*, *119*, 123–137. https://doi.org/10.1002/2013JF002759
Hamamori, A (1962). A theoretical investigation on the fluctuations of bed load transport (Technical Report Report R4). Netherlands: Delft Hydraulics Laboratory.
Hoey, T. B., & Sutherland, A. J. (1991). Channel morphology and bedload pulses in braided rivers: A laboratory study. *Earth Surface Processes and Landforms*, *16*(5), 447–462.
Iseya, F., & Ikeda, H. (1987). Pulsations in bedload transport rates induced by a longitudinal sediment sorting: A flume study using sand and gravel mixtures. *Geografiska Annaler. Series A, Physical Geography*, *69*, 15–27.
Jerolmack, D. J., & Paola, C. (2010). Shredding of environmental signals by sediment transport. *Geophysical Research Letters*, *37*, L19401. https://doi.org/10.1029/2010GL044638
Keylock, C. J., Lane, S. N., & Richards, K. S. (2014). Quadrant/octant sequencing and the role of coherent structures in bed load sediment entrainment. *Journal of Geophysical Research: Earth Surface*, *119*, 264–286. https://doi.org/10.1002/2012JF002698.
Lanzoni, S. (2000). Experiments on bar formation in a straight flume. 1. Uniform sediment. *Water Resources Research*, *36*, 3337–3349.
Lisle, T. E. (2004). Sediment wave. In A. Goudie (Ed.), *Encyclopedia of geomorphology* (Vol. 2, pp. 938). London: Routledge.
Martin, R., Jerolmack, D., & Schumer, R. (2012). The physical basis for anomalous diffusion in bed load transport. *Journal of Geophysical Research*, *117*, F01018. https://doi.org/10.1029/2011JF002075
Radice, A., Ballio, F., & Nikora, V. (2009). On statistical properties of bed load sediment concentration. *Water Resources Research*, *45*, W06501. https://doi.org/10.1029/2008WR007192
Recking, A., Frey, P., Paquier, A., & Belleudy, P. (2009). An experimental investigation of mechanisms involved in bed load sheet production and migration. *Journal of Geophysical Research*, *114*, F03010. https://doi.org/10.1029/2008JF000990
Redolfi, M., Bertoldi, W., Tubino, M., & Welber, M. (2018). Bed load variability and morphology of gravel bed rivers subject to unsteady flow: A laboratory investigation. *Water Resources Research*, *54*, 842–862. https://doi.org/10.1002/2017WR021143
Roseberry, J., Schmeeckle, M., & Furbish, D. (2012). A probabilistic description of the bed load sediment flux: 2. Particle activity and motions. *Journal of Geophysical Research*, *117*, F03032. https://doi.org/10.1029/2012JF002353
Saletti, M., Molnar, P., Zimmermann, A., Hassan, M. A., & Church, M. (2015). Temporal variability and memory in sediment transport in an experimental step-pool channel. *Water Resources Research*, *51*, 9325–9337. https://doi.org/10.1002/2015WR016929
Simons, D. B., Richardson, E. V., & Nordin, C. F. (1965). Bedload equation for ripples and dunes (Techical Report Professional Paper 462 H). US: U.S. Geological Survey.
Singh, A., Fienberg, K., Jerolmack, D., Marr, J., & Foufoula-Georgiou, E. (2009). Experimental evidence for statistical scaling and intermittency in sediment transport rates. *Journal of Geophysical Research*, *114*, F01025. https://doi.org/10.1029/2007JF000963
Turowski, J. (2010). Probability distributions of bed load transport rates: A new derivation and comparison with field data. *Water Resources Research*, *46*, W08501. https://doi.org/10.1029/2009WR008488
Visconti, F., Stefanon, L., Camporeale, C., Susin, F., Ridolfi, L., & Lanzoni, S. (2012). Bed evolution measurement with flowing water in morphodynamics experiments. *Earth Surface Processes and Landforms*, *37*, 818–827.
Wilson, G., & Hay, A. (2016). Acoustic observations of near-bed sediment concentration and flux statistics above migrating sand dunes. *Geophysical Research Letters*, *43*, 6304–6312. https://doi.org/10.1002/2016GL069579